MULTI-CHANNEL CORRELATOR ARRAY-FED MICROWAVE RADIOMETER

Jeffrey R. Piepmeier[1], Ali Mahnad[1,2], Giovanni De Amici[1], Jinzheng Peng[1,3], Jared Jordan[4], Ken Vanhille[4], Thomas Holmes[1], Paul Racette[1], Rafael Rincon[1]

[1]NASA's Goddard Space Flight Center, Greenbelt, MD 20771 USA, [2]Science Systems and Applications, Inc., Lanham, MD 20706 USA, [3]Universities Space Research Association, Columbia, MD 21044 USA, [4]Nuvotronics, Inc., Durham, NC 27703

ABSTRACT

Multiband passive microwave imagery in X to W Bands has a nearly 40-year history of utilization for measurement of multiple geophysical parameters (e.g., precipitation rate, ocean surface wind speed, sea ice concentration, and land surface temperature). Spatial resolution is limited by aperture size, and although aperture sizes have grown to 1-2 meters, current capability will not meet future spatial resolution needs. As aperture size increases, new antenna feed techniques are needed to maintain contiguous coverage and obtain Nyquist sampling. Here we apply the correlator array-fed radiometer architecture adapted from radio astronomy and show how it can meet emerging needs. Simulation results of a 0.8-m, 36.5-GHz, array-fed reflector (equivalent to 20 meters at 1.41 GHz) show the feasibility of creating multiple over-lapping beams.

Index Terms— Microwave radiometer

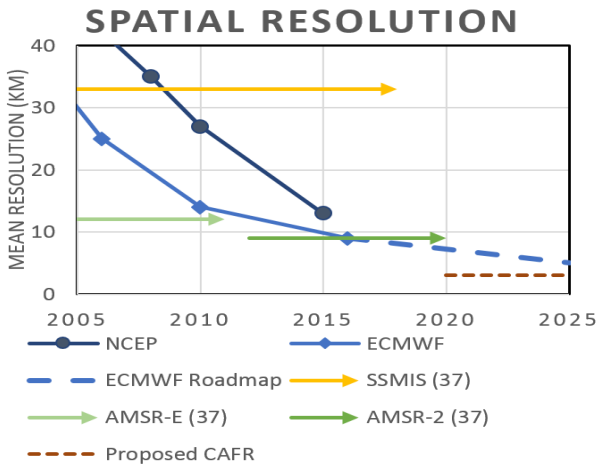

Fig.1. Historical development in mean spatial resolution of PMW radiometers (at 37 GHz), compared to operational analysis at numerical weather prediction centers. The dashed line indicates the proposed CAFR capability, which is needed to meet scientific and modeling needs.

1. INTRODUCTION

A. Emerging Need

Microwave radiometers are the work-horse of microwave remote sensing for Earth system science and have been so for almost 4 decades. Since 1987 multiple agencies, including NASA, USAF, and JAXA, have created a contiguous record of passive microwave (PMW) measurements with a core set of channels spanning K-band (18.7 or 19.5 GHz), Ka-band (36-37 GHz), to W-band (85-92 GHz) [1]-[6]. Later model instruments include X-band (10.7 GHz). Applications for the X- through W-band channels are many and include measurement of precipitation rate, sea ice concentration and snow water equivalent.

An emerging application is the use of PMW based estimates of land surface temperature (LST) as input to evapotranspiration (ET) retrievals [7]. This terrestrial application is currently dominated by thermal infrared technology due to the low spatial resolution (>10 km) of PMW sensors. Global estimates of ET are needed to (1) better monitor changes in water use in response to changing climate, land use, and population, (2) analyze crop water productivity, and (3) constrain the latent heat flux in hydrologic and numerical weather prediction models.

Historically, the low spatial resolution of PMW sensors (compared to visible and infrared imagery) was less of an issue when global weather models processed information at horizontal grid spacing of 40 km or more. But an exponential increase in computer power has led to a reduction in model grid spacing. As an illustration, the European Center for Medium-range Weather Forecasting (ECMWF) progressively increased the spatial resolution of its Integrated Forecasting System from 40 km in 2003 to 9 km in 2016. For 2025, the target is a horizontal resolution of 5 km [8]. In parallel to this, radiometer designers have achieved finer spatial resolution through an increase in aperture size, e.g.

growing from 0.6 m (TMI, SSM/I) to 1.6 m (AMSR-E) and 2.0 m (AMSR2). This larger aperture has allowed the footprint size of the higher frequency channels to match the increasing spatial resolution of the weather centers (see Fig. 1). To meet future needs the radiometer reflector needs to grow to 4-6 meters, which is 2-3 times larger than AMSR2.

B. Technical Dilemma

As science needs drive radiometer designers to utilize larger apertures, compromises are made to balance the spatial resolution-NEDT tradeoff (radiometric uncertainty principal) and SWaP resources. With only one beam, improving spatial resolution by making the antenna larger increases noise and/or creates gaps in imagery. The antenna spin rate could be slowed to allow for more integration time over a footprint, which improves NEDT; however, a slower spinning antenna will cause coverage gaps to appear on the ground. Thus, improving spatial resolution beyond today's capability will require multiband radiometers to have multiple beams at each frequency.

Furthermore, overlap between footprints is necessary for Nyquist sampling [12][13], especially when using image processing analysis (e.g., finding the location of the sea ice edge) or using spatial resampling algorithms [14]. While the small aperture of SSM/I and SSMIS provides at least 50% footprint overlap for frequencies up to Ka-band, today's larger-aperture imagers only provide Nyquist sampling for the lowest frequencies. For example, GMI only provides 50% footprint overlap at X-band while at Ka- and W-band the reflector is significantly under illuminated to broaden the beams and minimize the gaps between scans [6]. In other words, the design does not take advantage of the full aperture size to obtain the sharpest available resolution, which is traded against spatial under-sampling. If enough beams are available, the imager can take advantage of the full aperture size for all frequency channels, providing the sharpest possible resolution and maintain NEDT. Furthermore, if enough beams are distributed in the elevation direction, the azimuthal rotation rate of the reflector can even be lowered to increase integration time buying back NEDT as well as reducing spun momentum.

2. TECHNICAL APPROACH

A. Borrowed from Radio Astronomy

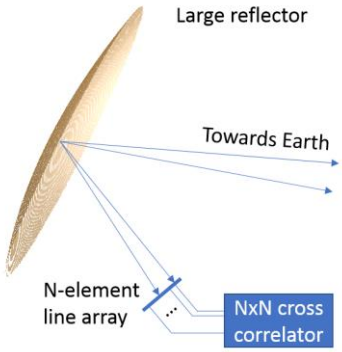

Fig.2. Multiple beams are generated in ground processing using a correlator array-fed reflector.

The array-fed radio telescope architecture was developed over previous decades and an L-band phased array feed was recently put into operation at Greenbank Telescope [15]. We borrow this architecture, adapting it to scanning radiometers, to produce a multibeam radiometer with contiguous coverage and overlapping footprints. In an offset-fed reflector configuration, the feed array is "excited" to create multiple virtual feeds with various distances from the focal point – see Fig.2.

We are developing a laboratory instrument to demonstrate the utility of the array-fed architecture at 36 GHz using an 80-cm projected aperture. The feed array is an 11-element line array based on "A Microfabricated 8-40 GHz Dual-Polarized Reflector Feed" [16]. By exciting groups of 6 elements each separated by one element spacing within the line array, multiple beams are generated pointing in slightly different directions. The simulated 3-dB contours of the 6 available main beams are shown in Fig. 3. Note how each beam is overlapped by half a beamwidth.

B. Correlator Array Equivalency

The simulated antenna patterns were generated using a phased-array of line elements for each virtual feed. Another approach is to use a correlator array, which for measuring power is equivalent to a phased array. Consider a two-element array with output voltages v_1 and v_2. The power received by a conventional beamformer with weights w_1 and w_2 is:

$$P = \langle |wv^T|^2 \rangle$$

where $w = [w_1 \quad w_2]$ and $v = [v_1 \quad v_2]$.

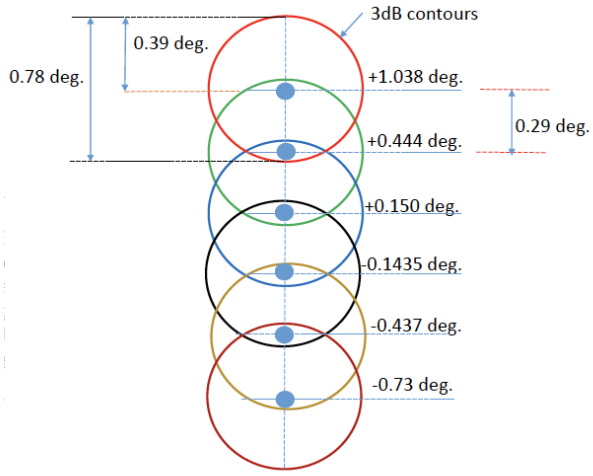

Fig.3. Multiple beams are generated by exciting 6 overlapping groups of 6 elements each in the 11-element line array fed reflector. The 3-dB contours overlap by slightly more than one-half of a beamwidth and scan by more than two beamwidths about the focal direction.

which can be rearranged, assuming the weights are constant and the voltages are wide-sense stationary random processes, to yield

$$P = WV^T$$

where $W = w \otimes w^*$ and $V = \langle v \otimes v^* \rangle$. The outer-product V is what would be measured by a cross-correlator:

$$V = [\langle |v_1|^2 \rangle \quad \langle v_1 v_2^* \rangle \quad \langle v_1^* v_2 \rangle \quad \langle |v_2|^2 \rangle]$$

Thus, the beams can be formed by linear combinations of cross-correlator output. A main advantage of this approach is the beamforming operation can be recomputed offline by simply changing the weights for calibration or optimization.

3. Envisioned System

We envision a multi-beam multi-frequency (X-W bands) conical scanning microwave radiometer with a 6-meter main reflector capable of spatial Nyquist sampling the Earth scene from LEO. The goals of the objective system include 95% beam efficiency and 20 dB mainlobe integrated cross-polarization. We utilize a multiband correlator array-fed architecture to realize multiple simultaneous beams, which are required to meet NEDT and spatial sampling requirements. To generate multiple footprints through an offset paraboloid main reflector, the array synthesizes apertures at multiple frequencies with different phase centers spaced in elevation about the focal point. Since beam forming is performed in ground processing, antenna calibration coefficients can be adjusted *post hoc* providing opportunity for beam matching, optimizing signal to noise and image processing. Integrated low noise amplifiers (LNAs) can be placed close to each line element. Using a wideband array also allows the designer to synthesize feeds at each frequency band occupying the same real estate about the focal point, thus permitting co-alignment of beams at each frequency.

Performance for an objective system at 700-km altitude (like AMSR2) is given in Table I. For a 6-m antenna rotating at 14.9 rpm (like SMAP), there is a 27-km gap between scans along the sub-satellite track. For each band, the major and minor axes of the instantaneous field-of-view (IFOV) are given. The number of footprints between scans is also given. A conventional antenna with a feed cluster would need 28 feed horns to achieve 3-dB edge-to-edge coverage and nearly twice as many for 50% overlap. We assume the W-band feed will under-illuminate the reflector for an effective 3-meter diameter. This assumption is made to mitigate the technical risks associated with the future development

Table I. *Performance goals for an objective 6-meter multiband radiometer.*

Frequency	**GHz**	**10.65**	**18.7**	**23.8**	**36.5**	**89.0**
Diameter	m	6	6	6	6	3
3dB beamwidth	deg	0.36	0.20	0.16	0.10	0.09
IFOV minor-axis	km	7.1	4.0	3.2	2.1	1.7
IFOV major axis	km	12.5	7.1	5.6	3.7	3.0
# IFOV's cross-scan		2.2	3.8	4.9	7.4	9.1
IF Bandwidth	MHz	100	200	400	1000	6000
Integration time	ms	2.69	1.53	1.20	0.79	0.65
NEDT goal	K	0.9	0.9	0.7	0.7	0.5

of a large mesh reflector operating at W-band. The SMAP 6-meter radiometer [9][10] demonstrated such an aperture size is dynamically feasible and there is work on-going to extend deployable RF capability to W-band [11][17].

4. Discussion

The array-fed architecture for microwave radiometers has the potential to solve the developing need for high-spatial resolution, large aperture instruments. Simulations of a 36.5 GHz system demonstrate the capability to synthesize multiple, overlapping, beams using a line-array feed. Using a correlator array receiver allows beamforming to be computed, and recomputed, after the fact for tailored performance and calibration. With continued technology development, the correlator array fed radiometer can be ready to meet the high-spatial resolution needs of emerging science and modelling capability.

References

[1] J. P. Hollinger, J. L. Peirce, and G. A. Poe, "SSM/I instrument evaluation," *IEEE Trans. Geosci. Remote Sens.*, vol. 28, no. 5, pp. 781–790, Sep. 1990.

[2] C. Kummerow, W. Barnes, T. Kozu, and J. Simpson, "The Tropical Rainfall Measuring Mission (TRMM) sensor package.," *J. Atmospheric Ocean. Technol.*, vol. 15, pp. 809–817, 1998.

[3] C. L. Parkinson, "Aqua: An Earth-observing satellite mission to examine water and other climate variables," *Geosci. Remote Sens. IEEE Trans. On*, vol. 41, no. 2, pp. 173–183, 2003.

[4] N. Sun and F. Weng, "Evaluation of special sensor microwave imager/sounder (SSMIS) environmental data records," *Geosci. Remote Sens. IEEE Trans. On*, vol. 46, no. 4, pp. 1006–1016, 2008.

[5] A. Okuyama and K. Imaoka, "Intercalibration of Advanced Microwave Scanning Radiometer-2 (AMSR2) Brightness Temperature," *IEEE Trans. Geosci. Remote Sens.*, vol. 53, no. 8, pp. 4568–4577, Aug. 2015.

[6] D. W. Draper, D. A. Newell, F. J. Wentz, S. Krimchansky, and G. M. Skofronick-Jackson, "The Global Precipitation Measurement (GPM) Microwave Imager (GMI): Instrument Overview and Early On-Orbit Performance," *IEEE J. Sel. Top. Appl. Earth Obs. Remote Sens.*, vol. 8, no. 7, pp. 3452–3462, Jul. 2015.

[7] T. R. Holmes, C. Hain, W. T. Crow, M. C. Anderson, and W. P. Kustas, "Microwave implementation of two-source energy balance approach for estimating evapotranspiration," *Hydrol. Earth Syst. Sci. Discuss.*, pp. 1–25, Jun. 2017.

[8] ECMWF, "ECMWF Roadmap to 2025," ECMWF, Reading, UK, 2016.

[9] J. R. Piepmeier *et al.*, "SMAP L-band Microwave Radiometer: Instrument Design and First Year on Orbit," *IEEE Trans. Geosci. Remote Sens.*, 2017.

[10] P. Focardi, M. W. Spencer, and J. R. Piepmeier, "SMAP instrument antenna, on orbit performance validation verification," in *2016 IEEE International Symposium on Antennas and Propagation (APSURSI)*, 2016, pp. 1371–1372.

[11] M. Klein, "Deployable microwave antennas for CubeSats, NanoSats, and SmallSats." Boulder Environmental Sciences and Technology, NASA SBIR 171 S1.02-9097, 2017.

[12] R. N. Bracewell, "Two-dimensional aerial smoothing in radio astronomy," *Aust. J. Phys.*, vol. 9, no. 3, pp. 297–314, 1956.

[13] N. Skou, "On The Sampling In Imaging Microwave Radiometers," in *International Geoscience and Remote Sensing Symposium*, 1988, pp. 17–18.

[14] D. G. Long and M. J. Brodzik, "Optimum image formation for spaceborne microwave radiometer products," *IEEE Trans. Geosci. Remote Sens.*, vol. 54, no. 5, pp. 2763–2779, 2016.

[15] D. Roshi, *et al.*, "Performance of a Highly Sensitive, 19-element, Dual-polarization, Cryogenic L-band Phased-array Feed on the Green Bank Telescope," *Astronomical J.*, vol.155, no.5, pp. 202-220, May 2018.

[16] Vanhille, *et al.*, "A Microfabricated 8-40 GHz Dual-Polarized Reflector Feed," *Antenna Applications Symposium*, 23-25 Sept. 2014; Monticello, IL. NASA Tech. Rep. 20140017771.

[17] G. Marks, E. Keay, S. Kuehn, M. Fedyk, and P. Laraway, "Performance of the astromesh deployable mesh reflector at ka-band frequencies and above," in *Fifteenth KA and Broadband Communications, Navigation and Earth Observation Conference*, 2009.